Effect of Reactor Configuration on Nitric Oxide Conversion in Nitrogen Plasma

Gui-Bing Zhao, S. V. B. Janardhan Garikipati, Xudong Hu, Morris D. Argyle, and Maciej Radosz
Dept. of Chemical and Petroleum Engineering, University of Wyoming, Laramie, WY 82071

DOI 10.1002/aic.10451
Published online April 4, 2005 in Wiley InterScience (www.interscience.wiley.com).

The configuration of a nonthermal plasma reactor strongly affects the rate of electron collision reactions. Experiments involving the decomposition of NO in N_2 were performed in a reactor in which the number of parallel reactor tubes varied from 1 to 10 at a constant pressure of 147.6 kPa and ambient temperature. A previously developed lumped model of the reactions accurately predicted the effects of varying the initial concentrations of NO (from 240 ppm to 593 ppm) and gas residence time (from 1.93 to 7.42 s). With an increasing number of parallel reactor tubes, the rate of electron collision reactions decreases because the energy input per unit reactor volume at unit time decreases, while the energy consumption per molecule of NO converted to N_2 and O_2 decreases due to electrical and geometric effects associated with the decreasing peak width of the discharge voltage pulses and increasing reactor capacitance. Therefore, increasing the number of parallel reactor tubes provides a viable scale-up method for constructing more efficient pulsed corona discharge reactors. © 2005 American Institute of Chemical Engineers
AIChE J, 51: 1813–1821, 2005
Keywords: pulsed corona discharge reactor, energy consumption, NO, configuration, scale-up

Introduction

The conversion of nitrogen oxides (NO_x) into elemental oxygen and nitrogen has become a central scientific concern because of the key role of NO_x in many global environmental problems, such as acid rain, photochemical smog formation and the greenhouse effect. These environmental concerns have resulted in considerable political pressure for the adoption of increasingly stringent NO_x emission standards. Among the emerging technologies for NO_x decomposition, nonthermal plasma is one of the most promising. A pulsed corona discharge reactor (PCDR) is a nonthermal plasma technology characterized by low gas temperature and high electron temperature achieved by producing high energy electrons in the gas while leaving the bulk temperature of the gas unchanged. A PCDR utilizes a high-voltage, short-duration (< 100 ns) electrical discharge between nonuniform electrodes to produce streamers through the growth of electron avalanches formed by electron collision ionization events in the gas.[1] A streamer is a region of highly ionized gas where a wide range of active radicals and chemical species are formed through electron collision reactions with the background gas. These active species, in turn, initiate bulk phase reactions that lead to NO_x conversion.

A critical issue in the use of plasma reactors for the treatment of NO_x is the energy consumption. The reported energy costs of using nonthermal plasmas for NO_x conversion vary considerably — for example, from 70 to 780 eV/molecule.[2] These conversions are characterized by low energy efficiency because N atoms, which are one of the main active species responsible for NO_x conversion, can be formed from N_2 dissociation at a low dissociation energy of 9.8 eV. One of the primary factors affecting energy consumption of NO_x conversion in nonthermal plasma reactors is the reactor configuration. Although many investigators[3-5] have recognized that reactor design is an important parameter for reducing energy cost in the conversion of NO using nonthermal plasma reactors, relatively few reports in the literature discuss reactor optimization. McLarnon and Penetrante[6] investigated the effect of packing materials, voltage frequencies and electrode diameter on NO conversion in

Correspondence concerning this article should be addressed to M. Radosz at radosz@uwyo.edu.

N_2 using a co-axial wire cylinder dielectric-barrier discharge reactor. They observed that reactor design had no substantial effect on energy consumption. Penetrante et al.[7] investigated and compared the electrical energy consumption of three different kinds of nonthermal plasma reactors: pulsed corona, dielectric-barrier discharge and dielectric pellet bed reactors. They observed that the radical production efficiency in these reactors cannot be enhanced by varying the voltage pulse parameters, using a dielectric barrier, adding a dielectric packing or changing the electrode structure. The measured energy consumption was 240 eV per NO molecule in their experiments. Namihira et al.[8] investigated the influence of reactor length on NO removal using a PCDR. They found that the energy efficiencies of both NO and NO_x decomposition slightly increase with reactor length, but are not strongly dependent on it. Recently, Zhao et al.[9] investigated the effects of series and parallel operation of multiple PCDRs on energy consumption during N_2O conversion. They found that series reactors are more energy efficient than a single reactor and parallel reactors.

For industrial applications of PCDRs, an important issue is scale-up in order to achieve maximum NO_x conversion efficiency at minimum energy consumption. The scale-up of conventional reactors can generally be achieved by simply enlarging the reactor. For nonthermal plasma reactors, like the PCDR, the reactor would cease to operate if the reactor size were increased by increasing tube diameter because the electrical discharge would no longer occur unless the voltage was increased. The only practical way to scale-up a PCDR is to increase the number of parallel reactor tubes, which may change the rate of electron collision reactions and affect the energy efficiency of NO_x conversion. However, no detailed studies have been conducted to explore these issues. The goal of this work is to understand the effect of the number of parallel reactor tubes used in a PCDR on electrical discharge, the rate of electron collision reactions and energy consumption using the reaction system of NO in N_2.

Experimental

The pulsed corona discharge reactor used in this work consisted of a high-voltage power supply with a control unit and the pulser/reactor assembly, as explained in detail elsewhere.[10] The high voltage controller contained the electronic and gas controls required to regulate the high voltage charging power supply, as well as the pulsed power delivered to the reactor gas. The charging capacitance C_P is fixed at 800 pF. The pulser/reactor assembly contained the pulsed power generator and the pulsed corona discharge reaction chambers. The reactor had 10 parallel reaction tubes, each 914 mm in length and 23 mm in dia., with a stainless steel wire, 0.58 mm in dia., passing axially through the center of each tube. The wire was positively charged, and the tube was grounded. The gas flowing through the reactor tube was converted to plasma by high voltage discharge from the reactor anodes. One tube was fitted with UV-grade quartz windows for diagnostics and plasma observation. The number of parallel-reactor tubes used in a given experiment was varied by installing a wire in the center of each active tube and sealing the unused tubes with Teflon corks with O-rings. The corona power per pulse was calculated from the product of the measured pulse voltage (V) and current (I). The energy delivered to the reactor per pulse is the time integral of power ($\int$VIdt). The power consumed W was calculated as the product of the input energy per pulse and the pulse frequency. The system design permitted variation and measurement of applied voltage and its frequency, reactor current and reactor voltage.

Table 1. Experimental Matrix

Reactor Tube Number	System	Flow Rate (m^3/s)	Gas Residence Time (s)
1	595 ppm NO + N_2	2.01×10^{-4}	1.89
	240 ppm NO + N_2	1.11×10^{-4}	3.42
2	595 ppm NO + N_2	1.02×10^{-4}	7.45
	595 ppm NO + N_2	2.19×10^{-4}	3.47
	595 ppm NO + N_2	3.94×10^{-4}	1.93
4	593 ppm NO + N_2	2.10×10^{-4}	7.23
6	593 ppm NO + N_2	2.55×10^{-4}	8.93
8	593 ppm NO + N_2	2.60×10^{-4}	11.7
10	593 ppm NO + N_2	3.70×10^{-4}	10.3

The experimental test matrix is shown in Table 1. The test gas mixture of NO in N_2 was introduced into the PCDR at ambient temperature, around 300 K, and at constant pressure, 147.6 kPa. The gas samples were collected from a common header at the discharge end of the PCDR in small stainless steel cylinders and analyzed for stable species using a Spectrum 2000 PerkinElmer Fourier transform infrared spectrometer with a narrow-band mercury cadmium telluride detector.

The energy consumption analysis of the PCDR was one of the main tasks in this work. The voltage and current pulses were the source of energy for the gas. For these experiments, the energy per pulse was about 0.192 J. As found previously,[11] NO_2 and N_2O are formed as byproducts when NO is converted in N_2. Therefore, total NO_x conversion was calculated, rather than NO conversion, because total NO_x conversion reflects the degree of direct decomposition of NO into N_2 and O_2. The total NO_x conversion was defined as the amount of NO converted to N_2, as follows

$$NO \rightarrow NO_2 + N_2O + N_2 + O_2 \quad (1)$$

$$X_{N_2} = \frac{C_{i,NO} - C_{o,NO} - C_{o,NO_2} - 2 \times C_{o,N_2O}}{C_{i,NO}} \times 100\% \quad (2)$$

The corresponding energy consumption En, in eV per NO molecule converted to benign gases (N_2 and O_2) is expressed below in terms of total NO_x conversion

$$En = \frac{W}{C_{i,NO} \cdot X_{N_2} \cdot F} \times 1.0364 \times 10^{-5} \quad (3)$$

In these equations, C_i is the concentration at the reactor inlet (mol/m^3), C_o is the concentration at the reactor outlet (mol/m^3), X_{N2} is the total conversion of NO to N_2, W is power input (J/s), F is flow rate (m^3/s), and 1.0364×10^{-5} is the conversion factor for J/mol to eV/molecule.

Mathematical Model

The pulsed corona discharge reactor described earlier was represented using a lumped kinetic model that describes the evolution of all species. The model details have been reported

Table 2. List of all Possible Chemical Reactions for Modeling the System NO in N_2

Chemical Reaction	Rate Constant ($cm^3 \cdot mol^{-1} \cdot s^{-1}$)	Source	No.
$N_2 + e \rightarrow N + N + e$	α_1 and β_1	This work	R1
$N_2 + e \rightarrow N_2(A) + e$	α_2 and β_2	This work	R2
$N + NO \rightarrow N_2 + O$	1.87×10^{13}	Atkinson et al.[25]	R3
$O + NO + N_2 \rightarrow NO_2 + N_2$	$k_0 = 3.62 \times 10^{16}$ $[N_2]$ $k_\infty = 1.81 \times 10^{13}$ $Fc = 0.85$	Atkinson et al.[26]	R4
$NO_2 + N \rightarrow N_2O + O$	1.81×10^{12}	Atkinson et al.[25]	R5
$NO_2 + N \rightarrow N_2 + O_2$	4.21×10^{11}	Kossyi et al.[27]	R6
$NO_2 + N \rightarrow N_2 + 2O$	5.48×10^{11}	Kossyi et al.[27]	R7
$NO_2 + N \rightarrow 2NO$	1.38×10^{12}	Kossyi et al.[27]	R8
$NO_2 + O \rightarrow NO + O_2$	5.85×10^{12}	Atkinson et al.[26]	R9
$N_2(A) + NO \rightarrow N_2 + NO$	3.31×10^{13}	Herron and Green[28]	R10
$N_2(A) + N_2O \rightarrow 2N_2 + O$	3.73×10^{12}	Herron and Green[28]	R11
$N_2(A) + NO_2 \rightarrow N_2 + NO + O$	7.83×10^{12}	Herron and Green[28]	R12
$N_2(A) + O_2 \rightarrow N_2 + 2O$	1.51×10^{12}	Herron and Green[28]	R13
$N_2(A) + O_2 \rightarrow N_2O + O$	4.70×10^{10}	Kossyi et al.[27]	R14
$N_2(A) + O_2 \rightarrow N_2 + O_2$	7.77×10^{11}	Kossyi et al.[27]	R15
$N_2(A) + O \rightarrow N_2 + O$	1.81×10^{13}	Herron and Green[28]	R16
$N_2(A) + N \rightarrow N_2 + N$	2.71×10^{13}	Herron and Green[28]	R17
$N + N + N_2 \rightarrow N_2 + N_2$	1.59×10^{15} $[N_2]$	Kossyi et al.[27]	R18
$O + O + N_2 \rightarrow O_2 + N_2$	1.10×10^{15} $[N_2]$	Kossyi et al.[27]	R19
$N + O + N_2 \rightarrow NO + N_2$	3.68×10^{15} $[N_2]$	Kossyi et al.[27]	R20

elsewhere,[12] and only a brief introduction is presented here. This model includes three main assumptions. (1) Electron-impact reactions occur during the entire residence time, both the pulse-on period and the pulse-off period, and, thus, the model represents a time average of the reactions; (2) The distribution function for electron velocity is Maxwellian. The rate constant for the electron-impact reaction $A + e \rightarrow B$ can then be expressed as

$$k[e] = \beta \sqrt{\frac{1}{\alpha P}}\, W^{0.75} \exp\left(-\frac{\alpha P}{W}\right) \tag{4}$$

where P is the system pressure, W is the power input and α and β are constants of proportionality, and (3) axial dispersion is negligible, and, hence, the gas flow can be considered as plug flow.

On the basis of these assumptions, a set of lumped model equations, including both electron-impact reactions and subsequent bulk reactions, were developed

$$\begin{cases} \dfrac{dC_1}{dt} = \displaystyle\sum_{j=1}^{M} \phi_{1j} \cdot r_j = g_1(C_1, C_2, \ldots, C_m; \alpha_1, \beta_1, \ldots, \alpha_n, \beta_n; W_k) \\ \dfrac{dC_2}{dt} = \displaystyle\sum_{j=1}^{M} \phi_{2j} \cdot r_j = g_2(C_1, C_2, \ldots, C_m; \alpha_1, \beta_1, \ldots, \alpha_n, \beta_n; W_k) \\ \qquad \ldots \quad \ldots \quad \ldots \quad \ldots \quad \ldots \\ \dfrac{dC_m}{dt} = \displaystyle\sum_{j=1}^{M} \phi_{mj} \cdot r_j = g_m(C_1, C_2, \ldots, C_m; \alpha_1, \beta_1, \ldots, \alpha_n, \beta_n; W_k) \end{cases} \quad (k = 1, 2, \ldots, L) \tag{5}$$

where C_i is the concentration of species i (i = 1, 2, . . ., m); t is time; M is the total number of reactions occurring in the PCDR including electron-impact reactions and subsequent bulk reactions; ϕ_{ij} is the stoichiometric coefficient of the i-th species in the j-th reaction; r_j is the reaction rate of the j-th reaction (j = 1, 2, · · · , M); n is the number of electron-impact reactions; α_j and β_j represent the model parameters for the j-th electron-impact reaction as shown in Eq. 4; and W_k (k = 1, 2, · · · , L) is the power input for the k-th experiment. Each experiment corresponds to a different concentration distribution in the reactor due to different power input. The model parameters α and β for electron-impact reactions were determined from experimental data using an optimization method.[12] On the basis of the prior work,[11,12] a total of 20 reactions with two electron collision reactions, shown in Table 2, were selected to simulate the system of NO in N_2.

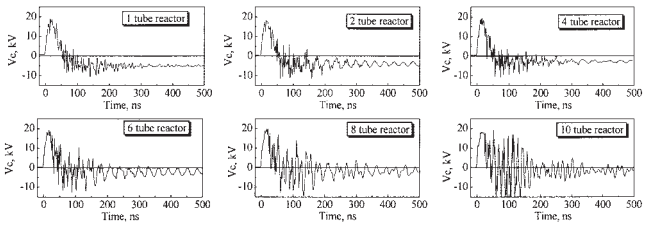

Figure 1. Effect of the number of parallel reactor tubes on the discharge voltage waveform at 200Hz.

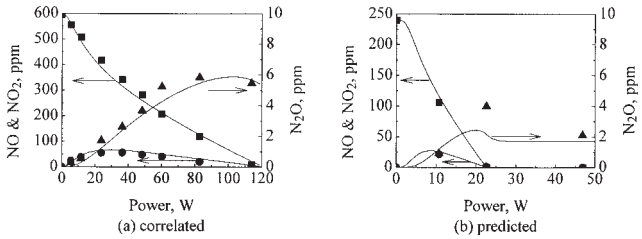

Figure 2. Lumped Model performance at different initial concentrations of NO in a one-tube reactor.

(a) 595 ppmNO + N_2; and (b) 240 ppmNO + N_2. Experimental data: ■ (NO), ● (NO_2), ▲ (N_2O); calculated data: —

Results and Discussion

The effect of the number of parallel reactor tubes on corona discharge

The important initiating reactions in the corona discharge are due to the collisions of the energetic electrons produced by the electrical discharge with gas molecules in the reactor. Therefore, the rate of electron collision reactions directly determines the rate of NO_x conversion. The fingerprint of the electron collision reactions in the PCDR is the discharge voltage vs. the time plot (waveform), which characterizes the properties of the streamers around the discharge wire. The main parameters that influence the properties of the streamers are the rise rate, pulse width and the peak value of the applied voltage.[13-16]

Figure 1 shows the discharge voltage waveforms for different numbers of parallel reactor tubes at 200 Hz and 147.6 kPa. The discharge voltage waveforms can be divided into two sections. The first section is the initial peak, where the discharge voltage increases from zero to a maximum and then decreases back to zero. Approximately 99% of the total energy to the PCDR is delivered in this first section, which corresponds to the energy dissipated for streamer propagation. The second section is the subsequent fluctuations of discharge voltage, which corresponds to the energy dissipated after streamer propagation. As discussed by Mok et al.[17] the second section of the energy input produces only slow electrons that do not contribute to the formation of active species because the energy delivered after streamer propagation is mainly used to sustain the low conductivity streamer channel and produce secondary streamers. Therefore, the important characteristics of the discharge streamer can be described by the first section of the discharge voltage. The important parameters of the first peak are the rise rate, pulse width and peak value of the applied voltage, which are shown in Table 3 for the different reactor configurations. These results show that pulse peak value and rise rate are not affected by the number of parallel reactor tubes. However, the pulse width decreases as the number of parallel reactor tubes increases. The pulse width is an important parameter that characterizes the energy efficiency of plasma chemical reactions. Generally, short pulses are more economical in energy cost than longer pulses.[4,13]

Table 3. Influence of Parallel Reactor Tube Number on Discharge Parameters at 200 Hz

Reactor Tube Number	Pulse Peak (kV)	Pulse Width (ns)	Rising Rate (kV/ns)
1	19.3	51	1.32
2	18.3	47	1.33
4	19.6	43	1.35
6	19.5	31	1.39
8	20.0	29	1.37
10	18.2	29	1.36

The effect of initial NO concentration and gas residence time on model parameters

Previous studies[12] using a four-tube reactor showed that the lumped model accurately predicts the effect of the inlet concentration of NO ranging from 593 ppm to 614 ppm, and the effect of gas residence time ranging from 3.63 s to 7.06 s for the reaction system of NO in N_2. In this work, we extended the range of experimental conditions. For example, the inlet concentration of NO varied from 593 ppm to 240 ppm and gas residence time varied from 1.93 s to 7.42 s to further verify the validity of the lumped model. If the lumped model accurately reflects the effect of the initial NO concentration and gas residence time, only one set of experimental data may be used to obtain the model parameters α and β for electron collision reactions R1 and R2. These values of α and β can then be used to model the energy consumption of NO decomposition at different initial NO concentrations and gas residence times for any number of parallel reactor tubes used.

Using the optimization method developed previously,[12] the experimental data with an initial NO concentration of 595 ppm in N_2 in a one-tube reactor determined the model parameters α and β for the electron collision reactions R1 and R2. The following model parameters were obtained

$$N_2 + e \rightarrow N + N + e \quad \beta = 1.09 \times 10^{-5} \quad \alpha = 3.68 \quad \text{(R1)}$$

$$N_2 + e \rightarrow N_2(A) + e \quad \beta = 1.68 \times 10^{-4} \quad \alpha = 5.10 \quad \text{(R2)}$$

Figure 2a shows the experimental and correlated values of NO_x at the reactor outlet. The calculated curves reasonably represent the experimental data. The same parameters were used to predict the experimental concentrations of all species for the inlet concentration of 240 ppm NO in N_2, as shown in Figure 2b. Although the N_2O fit is not precise due to the low concentration of N_2O, the model accurately predicts the maximum. The prediction of the trends in NO_x evolution for the experiment with 240 ppm NO in N_2 using the model parameters developed from the experiment with 595 ppm NO in N_2 shows that the lumped model captures the effect of varying the initial NO concentrations.

Using the optimization method developed previously,[12] the experimental data at the gas flow rate of 1.024×10^{-4} m^3/s in

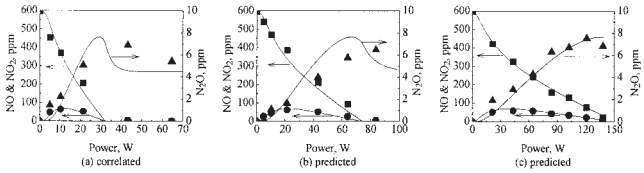

Figure 3. Lumped Model performance at different gas flowrates in two-tube reactor.

(a) 1.024×10^{-4} m^3/s, (b) 2.191×10^{-4} m^3/s, and (c) 3.943×10^{-4} m^3/s. Experimental data: ■ (NO), ● (NO_2), ▲ (N_2O); Model calculated data: —

a two-tube reactor (corresponding to gas residence time of 7.42 s) are used to determine the model parameters α and β of electron collision reactions R1 and R2. The following model parameters were obtained

$$N_2 + e \rightarrow N + N + e \quad \beta = 9.79 \times 10^{-6} \quad \alpha = 3.88 \quad \text{(R1)}$$

$$N_2 + e \rightarrow N_2(A) + e \quad \beta = 7.37 \times 10^{-5} \quad \alpha = 4.94 \quad \text{(R2)}$$

Figure 3a shows the experimental and correlated values of NO_x at the reactor outlet. The calculated curves again reasonably represent the experimental data. The same parameters were used to predict the experimental results for two other flow rates, 2.191×10^{-4} m^3/s and 3.943×10^{-4} m^3/s, which correspond to gas residence times of 3.47 s and 1.93 s, respectively. Figures 3b and 3c show the experimental and predicted values for these two different flow rates. The reasonable prediction of NO_x evolution for different gas residence times using one set of parameters shows that the lumped model captures the effect of varying gas residence times and proves that the assumption of plug flow in the lumped model is valid.

The effect of the number of parallel reactor tubes on the rates of electron collision reactions

Because the pulse widths decrease with an increasing number of parallel reactor tubes (Table 3), it appears that the number of parallel reactor tubes affects the rate of electron collision reactions. The important model parameters embodying the rate of electron collision reactions are α and β, as shown in Eq. 4. The method used to determine the model parameters of electron collision reactions R1 and R2 for one- and two-tube reactors was discussed previously. The same method[12] was used to determine model parameters of the electron collision reactions R1 and R2 for four-, six-, eight- and 10-tube reactors. Figure 4 shows the experimental data and the correlated data for NO, NO_2 and N_2O concentrations at the reactor outlet. The similarity of the experimental data and the correlated data indicates that model parameters α and β of R1 and R2 characterize the kinetics of electron collision reactions.

Figures 2 – 4 show that there are always maximums in NO_2 and N_2O concentrations for a range of different initial concentrations of NO, gas residence times and the number of parallel reactor tubes, as shown in Table 1. The evolution of NO concentration is the result of two processes: a reduction process (reaction R3 in Table 2) and an oxidation process (reaction R4). As corona power input increases, more NO_2 is generated by reaction R4, which then leads to an increase in the rate of the

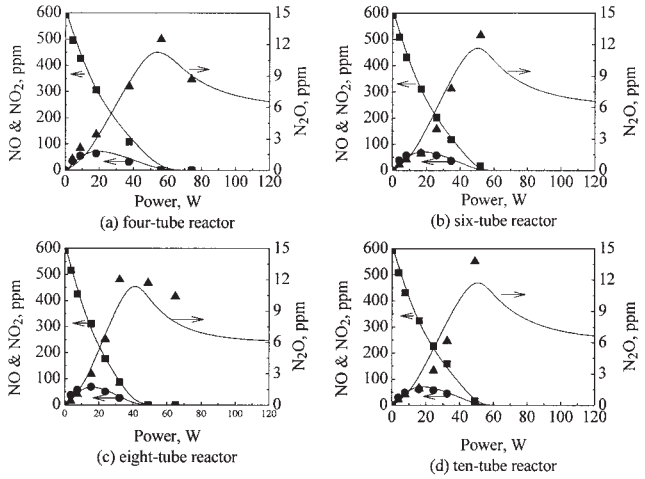

Figure 4. Experimental and correlated data for varying numbers of parallel reactor tubes.

(a) four-tube reactor, (b) six-tube reactor, (c) eight-tube reactor, and (d) 10-tube reactor. Experimental data: ■ (NO), ● (NO_2), ▲ (N_2O); calculated data: —

NO_2 conversion reactions R5–R9 and R12. As a result, NO_2 evolution reaches a maximum. N_2O is formed from reaction R5. $N_2(A)$, which is the first excited electronic state of nitrogen, is the only active species responsible for N_2O conversion, through reaction R11.[11] However, before NO is completely converted, $N_2(A)$ begins to be quenched by reaction R10 because its rate constant is 10 times higher than the rate constant of reaction R11. Therefore, the N_2O concentration increases with an increasing power input before NO is completely converted. After NO is completely converted, N_2O is converted by reacting with $N_2(A)$, which leads to the maximum N_2O concentration. At a higher power input, as shown in Figures 2b, 3a, 4b and 4c, the N_2O concentration reaches a stable value and cannot be further converted because the O_2, N and O formed from the complete conversion of NO and NO_2 strongly quench the active species $N_2(A)$ through reactions R13 – R17, as shown in Table 2. However, an important finding is that the maximum NO_2 concentration, the maximum N_2O concentration and the asymptotic value of N_2O concentration occur at the same values of the total NO_x conversion (30.9% ± 2%, 88.6% ± 3% and 98.5% ± 0.5%, respectively), which are independent of the initial concentration of NO, gas residence time and the number of parallel reactor tubes used. This observation suggests that the reaction mechanism is unaffected by the varying experimental parameters and further confirms that the lumped model is capable of representing the NO/N_2 system as described later.

Figure 5 shows the effect of the number of parallel reactor tubes on the model parameters for the two electron collision reactions R1 and R2. Previous work[12,18] has shown that the model parameter β includes the reactor and electrode geometry effects. For reaction R1, β decreases as the number of parallel reactor tubes increases. For reaction R2, β initially decreases but remains constant at higher tube numbers. This confirms the previous conjecture that β mainly depends on the reactor configuration. The model parameter α depends on the threshold ionization potential of the reactant gases[12,18] and, therefore, is

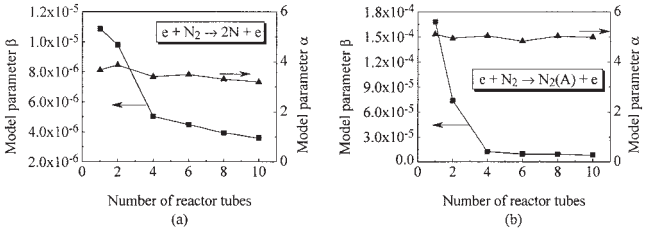

Figure 5. Effect of the number of parallel reactor tubes on model parameters α and β for two electron collision reactions.

(a) Electron collision reaction R1, and (b) Electron collision reaction R2. Data: ■ (β), ▲ (α).

almost independent of the number of parallel reactor tubes for the two electron collision reactions.

Figure 6 shows the variation of the rate constants of the electron collision reactions R1 and R2 as a function of the power input for different numbers of parallel reactor tubes. The rate constant of the electron collision reaction R1 decreases as the number of parallel reactor tubes increases at the same power input. The rate constant of the electron collision reaction R2 initially decreases as the number of parallel reactor tubes increases from one to four, and then reaches a stable value when there are more than six reactor tubes for a given power input. This confirms the previous conjecture that rate of electron collision reactions is reactor configuration dependent.[12,18] As shown in Eq. 4, the rate constant of electron collision reactions is governed by power input. The energy input to a unit reactor volume at unit time decreases with an increasing number of parallel reactor tubes, which explains why the rate of the electron collision reactions R1 and R2 decreases with the parallel reactor tube number at the same power input, as shown in Figure 6.

The effect of gas residence time and power input on energy consumption

The previous section shows that the lumped model captures the effect of the initial concentration of NO and gas residence time over the experimental range considered in this study. Also, the section on the rate of electron collision reactions shows that the model correlates well with the experimental results for the different reactor configurations achieved by changing model parameter β. Therefore, the lumped model can be used to investigate the conversion of NO and its energy consumption at different power inputs, initial NO concentrations and gas residence times. However, for convenience of comparison, a reaction system with the same initial concentration of ~600 ppm NO in N_2 was studied.

Figure 7 shows three-dimensional (3-D) plots of the conversion of NO (Figure 7a) and energy consumption (Figure 7b) as functions of power input and residence time for a four-tube reactor. Other reactor configurations generate similar plots. The model parameters α and β (shown in Figure 5) for the electron collision reactions R1 and R2 were used in the calculation. The fraction of NO converted to benign N_2 and O_2 is used to define NO conversion and energy consumption, as in Eqs 2 and 3. Figure 7a shows that the conversion of NO reaches a constant

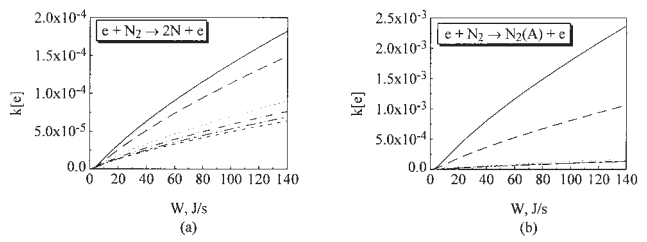

Figure 6. Rate constant of electron collision reaction as a function of power input for different number of parallel reactor tubes.

(a) Electron collision reaction R1, (b) Electron collision reaction R2. (— one-tube reactor; – – – two-tube reactor; · · · · · four-tube reactor; – · – · – six-tube reactor; – · · – eight-tube reactor; – 10-tube reactor).

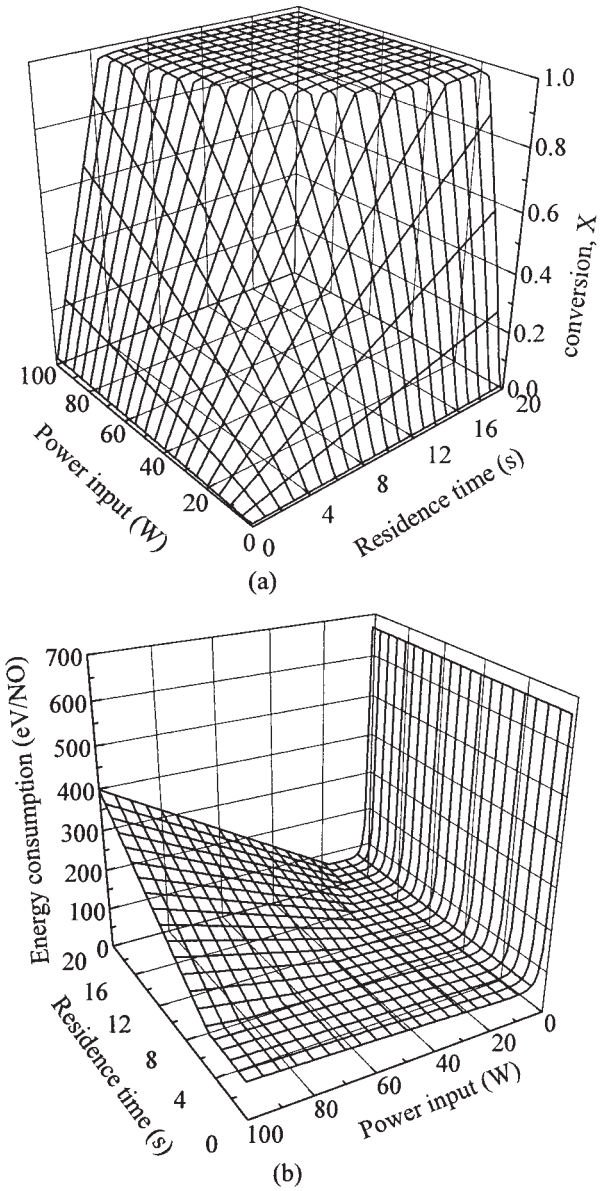

Figure 7. Effect of gas residence time and power input on energy consumption of NO conversion to N_2 and O_2 (four-tube reactor).

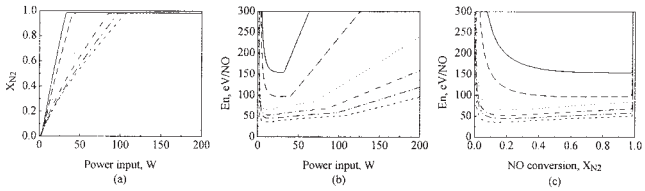

Figure 8. Effect of the number of parallel reactor tubes on energy consumption at a gas residence time of 6 s (— one-tube reactor; −−− two-tube reactor; · ·· ··· · four-tube reactor; − · − · − six-tube reactor; − ·· −eight-tube reactor; – 10-tube reactor).

value, around 98-99%, at higher power inputs and/or longer residence times because the byproduct N_2O is not fully converted to benign N_2 and O_2 in the reactor, as discussed previously.

Before NO conversion reaches the constant value, the energy consumption weakly increases with gas residence time at the same power input, as shown in Figure 7b. At a low power input, less than 5–10W, the energy consumption decreases quickly with an increasing power input at the same gas residence time. Before NO conversion reaches the plateau value at a high power input ($>$ 5–10W), the energy consumption weakly increases with the power input at the same gas residence time, which is mainly due to the continuous formation of byproduct N_2O through reaction R5. This indicates, as with N_2O conversion,[9] that an optimal power input corresponding to a minimal energy consumption exists for NO conversion at a given gas residence time. A similar conclusion can be drawn from the experimental data provided by Mizuno et al.[19]

In this work, highest space velocity (SV) of 1905 L/h (corresponding to gas residence time of 1.89 s) is used in the experiments. Typical plasma reactor SV for NO_x reduction chemistry is on the order of at least 100,000 L/h, and SV of over 750,000 L/h have shown quite interesting energy-destruction behavior. Further work is needed to examine the effect of reactor configuration on NO_x conversion at higher space velocities.

The effect of reactor tube number on energy consumption

The energy consumed depends on power input and residence time, both of which can be regulated to obtain optimum energy consumption for a particular reactor configuration. However, when the number of parallel reactor tubes changes, changing the reactor configuration, the energy efficiency also changes, and, hence, the energy consumption changes. Figure 8 shows the dependence of NO conversion (Figure 8a) and energy consumption (Figure 8b) on power input and the relation between energy consumption and NO conversion (Figure 8c) for different numbers of parallel reactor tubes at 147.6 kPa pressure and 6 s of gas residence time (corresponding to a gas flow rate of 6.33×10^{-4} $m^3 \cdot s^{-1}$ for the one tube reactor) at the same initial concentration of 600 ppm NO in N_2. The model parameters α and β (Figure 5) for electron collision reactions R1 and R2 were used in the calculation. NO conversion and the associated energy consumption were defined by Eqs. 2 and 3.

As shown in Figure 8a, NO conversion increases with power and then reaches a stable value, consistent with Figure 7a. However, with an increasing number of reactor tubes, NO conversion decreases for the same power input because the energy density decreases with the increase in reactor volume. With increasing power input, the energy consumption for NO conversion initially decreases quickly and then slowly increases, finally increasing linearly with power input, as shown in Figure 8b. The final linear increase of energy consumption with power input is associated with the production of N_2O, which cannot be converted into N_2 and O_2, as explained previously. The results show that there is an optimal power input corresponding to a minimal energy consumption, which indicates that operating conditions of the PCDR can be optimized in order to decrease energy consumption. Figure 8c shows that energy consumption decreases with an increasing NO conversion at conversions below ~20%. At intermediate conversions, the energy consumption is constant or slightly increases with increasing conversion. The sharp increase in energy consumption at high NO conversion (98-99%) is caused by the difficulty of converting byproduct N_2O. The minimum energy consumption per molecule of NO (~35 eV/molecule) for the 10-tube reactor is half of the lowest value reported previously[2] (70 eV/molecule). While this is still 3.6 times the theoretical minimum (9.8 eV/molecule for N_2 dissociation), ~35 eV/molecule is the most efficient value yet reported. Furthermore, the minimum energy/molecule value is fairly insensitive to increasing conversion (for example, ~50 eV/molecule at 98% NO conversion for the 10-tube reactor), which is again far superior to previous results.

Figures 8b and c show that at the same power input or the same NO conversion, the energy consumption of NO conversion decreases with an increasing number of parallel reactor tubes, which is shown explicitly in Figures 9a and b. Figures 9a and b show the energy consumption during NO conversion as a function of the number of parallel reactor tubes for different gas residence times at a constant power input (15 W) and constant NO conversion (90%). The consistent conclusion is that the increase in parallel reactor tube number (reactor volume) decreases the energy consumption for NO conversion. This implies that the scale-up of a PCDR can be achieved by increasing the number of parallel reactor tubes. The energy efficiency is increased during the scale-up process as a result of two factors. First, as shown in Table 3, the pulse width of the initial discharge voltage peak decreases with an increasing number of parallel reactor tubes (Figure 1). Namihira et al.[20] found that the energy required to convert NO decreased with a

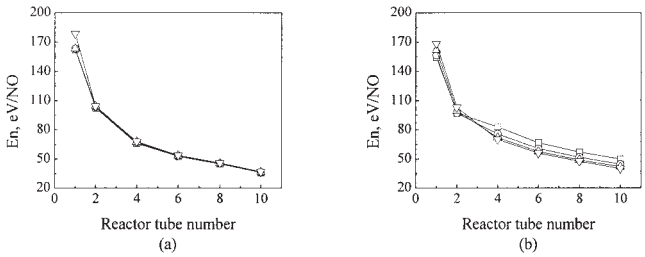

Figure 9. Energy consumption of NO conversion as a function of the number of reactor tubes.

(a) At power input of 15W, (b) At 90% conversion of NO gas residence time: □ 6s, ○ 9s, △ 12s, ▽ 15s.

decreasing pulse width because the interaction time of energetic electrons and gas molecules and the acceleration time of ions during short pulses are less than that for long pulses. Therefore, less energy is dissipated as heat, which increases the energy efficiency of plasma chemical reactions for shorter pulse widths.

In addition, Uhm and Lee[21] reported that the reactor capacitor plays a pivotal role for energy efficiency during NO conversion. Mok et al.[22] further found that when the pulse-forming capacitance (the capacitance of the charging capacitor, 800 pF for the reactors in our study) is five times larger than the geometric capacitance of the reactor, the energy utilization efficiency was maximized. Chung et al.[23] observed the maximum NO conversion efficiency when the pulse-forming capacitance is 3.4 times larger than the reactor capacitance. This indicates that NO conversion efficiency can be achieved by applying a low ratio of the pulse-forming capacitance to reactor capacitance, typically 3-5. The capacitance of a co-axial cylinder is defined as[24]

$$C = \frac{2\pi\varepsilon_0 L}{\ln(R/r)} \tag{6}$$

where ε_0 is the permittivity of N_2, l is the length of the reactor, R is the inner radius of the cathode (reactor tube), and r is the outer radius of the anode (central wire). Thus, one tube of this reactor has a capacitance of 13.9 pF. The capacitance of multiple parallel co-axial cylinder capacitors (C_N) is

$$C_N = NC \tag{7}$$

where N is the number of parallel reactor tubes. Therefore, with an increasing number of parallel reactor tubes, the reactor capacitance increases, allowing the external circuit to deliver energy to the reactor more efficiently, which is another reason for the observed decrease in energy consumption with an increasing number of parallel reactor tubes. The ratio of the pulse-forming capacitance (C_P) to reactor capacitance for our reactor configuration is

$$\frac{C_P}{C_N} = \frac{800}{13.9N} = \frac{57.8}{N} \tag{8}$$

Therefore, by increasing the parallel reactor tube number from one to 10, the ratio of the pulse-forming capacitance to the reactor capacitance decreases from 57.8 to 5.78, which is close to the optimal ratio of the pulse-forming capacitance to reactor capacitance as presented by Mok et al.[22] and Chung et al.[23]

Actual combustion exhaust streams contain percent levels of electronegative gases, such as O_2, CO_2 and H_2O, which have high electron affinities. Their presence can affect the electronic discharge because of electron attachment processes, which change the reaction chemistry dramatically, as reported by Zhao et al.[29-31] Therefore, further work is needed to examine the effect of reactor configuration on NO_x conversion at more representative feed compositions.

Conclusions

In this work, carefully designed experiments were conducted to investigate how the number of parallel reactor tubes affects the rate of electron collision reactions and energy efficiency for NO conversion in N_2. The pulse width of the initial discharge voltage peak decreases with an increasing number of parallel reactor tubes. The lumped model developed previously accurately models the effect of the initial concentration of NO and gas residence time, but it does not capture the effect of reactor configuration. Therefore, different model parameters are required for different reactor configurations. The rate of electron collision reaction decreases with an increasing number of parallel reactor tubes. The energy consumption of NO conversion weakly depends on gas residence time at a given power input. However, there is an optimal power input corresponding to a minimal energy consumption at a given gas residence time. The energy consumption during NO conversion decreases with increasing numbers of parallel reactor tubes at the same power input or at the same NO conversion. This indicates that the scale-up of PCDR can be achieved by increasing the number of parallel reactor tubes.

Acknowledgments

This work was funded by the National Science Foundation (CTS - 9810040; CTS - 0078700) and the Department of Defense (ARO-DAAD19-01-1-0488). The matching support was provided by the Research Office, University of Wyoming. The authors also gratefully acknowledge experimental assistance provided by Dr. S. Legowski and Mr. R. Borgialli.

Literature Cited

1. Raether H. Electron Avalanches and Breakdown in Gases. Washington: Butterworths, 1964.
2. Yamamoto T, Yang CL, Beltran MR, Kravets Z. Plasma-Assisted Chemical Process for NOx Control. *IEEE Trans Ind Appl.* 2000;36:923-927.
3. Tas MA, van Hardeveld R, van Veldhuizen EM. Reactions of NO in a positive streamer corona plasma. *Plasma Chem. Plasma Process.* 1997;17:371-391.
4. Puchkarev V, Gundersen M. Energy efficient plasma processing of gaseous emission using a short pulse discharge. *Appl. Phys. Lett.* 1997;71:3364-3366.
5. Yan K, Van Heesch EJM, Pemen AJM, Huijbrechts PAHJ. From chemical kinetics to streamer corona reactor and voltage pulse generator. *Plasma Chem. Plasma Process.* 2001;21:107-137.
6. McLarnon CR, Penetrante BM. Effect of reactor design on the plasma treatment of NOx 1998:SAE Technical Paper Series 982434.
7. Penetrante BM, Hsiao MC, Merritt BT, Vogtlin GE, Wallman PH. Comparison of Electrical Discharge Techniques for Nonthermal Plasma Processing of NO in N_2. *IEEE Trans Plasma Sci.* 1995;23:679-687.
8. Namihira T, Tsukamoto S, Wang D, Hori H, Katsuki S, Hackam R, Akiyama H, Shimizu M, Yokoyama K. Influence of Gas Flow Rate and Reactor Length on NO Removal Using Pulsed Power. *IEEE Trans Plasma Sci.* 2001;29:592-598.
9. Zhao G-B, Hu X, Plumb OA, Radosz M. Energy consumption and optimal reactor configuration for nonthermal plasma conversion of N_2O in nitrogen and N_2O in Argon. *Energy & Fuels.* 2004;18:1522-1530.
10. Hu X, Nicholas J, Zhang JJ, Linjewile TM, de Filippis P, Agarwal PK. The destruction of N_2O in a pulsed corona discharge reactor. *Fuel.* 2002;81:1259-1268.
11. Zhao G-B, Hu X, Argyle MD, Radosz M. N Atom and $N_2(A^3\Sigma_u^+)$ found to be responsible for nitrogen oxides conversion in nonthermal nitrogen plasma. *Ind Eng Chem Res.* 2004;43:5077-5088.
12. Zhao G-B, Hu X, Yeung MC, Plumb OA, Radosz M. Nonthermal plasma reactions of dilute nitrogen oxide mixtures: NOx in nitrogen. *Ind Eng Chem Res.* 2004;43:2315-2323.

13. Hackam R, Akiyama H. Air pollution control by electrical discharges. *IEEE Trans Dielectr Electr Insul.* 2000;7:654-683.
14. van Veldhuizen EM, Creyghton YLM, Rutgers WR. High Resolution Schlieren Study of Pulsed Corona *Proc. of 4th Int. Conf. on ESP*. Beijing, China, 1990.
15. Creyghton YLM, van Bladel FMAM, van Veldhuizen EM. Electrical and Spectroscopic Investigation of Pulsed Positive Streamer Corona in O_2-N_2 and CO_2-O_2 Mixtures *3rd Int. Symp. on High Pressure, Low Temperature Plasma Chemistry*. Strasbourg, France, 1991.
16. Creyghton YM, van Veldhuizen EM, Rutgers WR. Streamer characteristics of Positive Pulsed Corona *10th Int Symp on Plasma Chemistry*. Bochum, Germany, 1991.
17. Mok YS, Ham SW, Nam IS. Mathematical analysis of positive pulsed corona discharge process employed for removal of nitrogen oxides. *IEEE Trans Plasma Sci.* 1998;26:1566-1574.
18. Hu X, Zhang J-J, Mukhnahallipatna S, Hamann J, Biggs MJ, Agarwal P. Transformations and destruction of nitrogen oxides-NO, NO_2 and N_2O-in a pulsed corona discharge reactor. *Fuel* 2003;82:1675-1684.
19. Mizuno A, Shimizu K, Chakrabarti A, Dascalescu L, Furuta S. NOx removal process using pulsed discharge plasma. *IEEE Trans Ind Appl.* 1995;31:957-963.
20. Namihira T, Tsukamoto S, Wang D, Katsuki S, Hackam R, Akiyama H, Uchida Y, Koike M. Improvement of NOx removal efficiency using short-width pulsed power. *IEEE Trans Plasma Sc.* 2000;28:434-442.
21. Uhm HS, Lee WM. An analytical theory of corona discharge plasmas. *Phys Plasmas* 1997;4:3117-3128.
22. Mok YS, Ham SW, Nam IS. Evaluation of energy utilization efficiencies for SO_2 and NO removal by pulsed corona discharge process. *Plasma Chem Plasma Process.* 1998;18:535-550.
23. Chung JW, Cho MH, Son BH, Mok YS, Namkung W. Study on reduction of energy consumption in pulsed corona discharge process for NOx removal. *Plasma Chem Plasma Process.* 2000;20:495-509.
24. Shin DN, Park CW, Hahn JW. Detection of $OH(A^2\Sigma^+)$ and $O(^1D)$ emission spectrum generated in a pulsed corona plasma. *Bul. Korean Chem Soc.* 2000;21:228-232.
25. Atkinson R, Baulch DL, Cox RA, Hampson JRF, Kerr JA, Troe J. Evaluated kinetic and photochemical data for atmospheric chemistry: Supplement III. *J Phys Chem Ref Data.* 1989;18:881-1097.
26. Atkinson R, Baulch DL, Cox RA, Hampson JRF, Kerr JA, Rossi MJ, Troe J. Evaluated kinetic and photochemical data for atmospheric chemistry: Supplement VI. *J. Phys Chem Ref Data.* 1997;26:1329-1499.
27. Kossyi IA, Kostinsky AY, Matveyev AA, Silakov VP. Kinetic scheme of the non-equilibrium discharge in nitrogen-oxygen mixtures. *Plasma Sources Sci Technol.* 1992;1:207-220.
28. Herron JT, Green DS. Chemical kinetics database and predictive schemes for nonthermal humid air plasma chemistry. Part II. Neutral species reactions. *Plasma Chem Plasma Process.* 2001;21:459-481.
29. Zhao G-B, Garikipati SVBJ, Hu X, Argyle MD, Radosz M. Effect of oxygen on nonthermal plasma reactions of nitrogen oxides in nitrogen. *AIChE J* 2005;51(6):1800-1812.
30. Zhao G-B, Hu X, Argyle MD, Radosz M. Effect of CO_2 on nonthermal-plasma reactions of nitrogen oxides in N_2. 1. PPM-level concentrations. *Ind Eng Chem Res.* 2005;44: in press.
31. Zhao G-B, Hu X, Argyle MD, Radosz M. Effect of CO_2 on nonthermal-plasma reactions of nitrogen oxides in N_2. 2. Percent-level concentrations. *Ind Eng Chem Res.* 2005;44: in press.

Manuscript received May 25, 2004, and revision received Oct. 9, 2004.